SSRG International Journal of Electrical and Electronics Engineering
ISSN: 2348-8379/ https://doi.org/10.14445/23488379/IJEEE-V11I6P127

Volume 11 Issue 6, 250-258, Month 2024

Original Article

Distributed Secondary Control Using a Low Bandwidth Communication Channel to Enhance Voltage Regulation and Current Sharing Accuracy in DC Microgrid

Shilpa L. Kaila[1], Rajnikant H. Bhesdadiya[2], Hitesh M. Karkar[3]

[1] *Research scholar, Department of Electrical Engineering, Gujarat Technological University, Gujarat, India.*
[2]*Department of Electrical Engineering, Lukhdhirji Engineering College, Gujarat, India.*
[3]*Department of Electrical Engineering, Government Engineering College, Rajkot, Gujarat, India.*

[1]*Corresponding Author : Shilpakaila28@Gmail.Com*

Received: 12 April 2024 Revised: 15 May 2024 Accepted: 12 June 2024 Published: 29 June 2024

Abstract *- Now, DC microgrids are more popular due to their easier control, higher reliability, and efficiency. The main control objective of a DC microgrid is to achieve good voltage regulation and current-sharing accuracy simultaneously. Traditionally, for proper current sharing, droop control is used. However it suffers from poor voltage regulation with an increase in load due to droop action and reduces current sharing accuracy due to differences in line resistance. This paper presents a distributed secondary-level control using a Low-Bandwidth Communication (LBC) channel to overcome the limitations of a droop control and enhance the performance of a DC microgrid. It contains two secondary controllers, the average current controller and the voltage controller, to calculate current and voltage errors. This error is used to generate a voltage shifting term for simultaneously improving voltage regulation and current sharing accuracy, regardless of the different line resistances. This control handles both Constant Power Loads (CPLs) and resistive loads. It also validates the most important plug-and-play feature of a DC microgrid. MATLAB / simulation is utilized to validate the results of the presented control technique.*

Keywords *- Droop control, Voltage regulation, Current sharing, Microgrid, Distributed control.*

1. Introduction

Renewable energy resources such as solar, wind, and fuel cells have gained popularity recently in order to reduce the worldwide energy crises and severe environmental issues caused by the burning of fossil fuels. These sources are merged with the electrical grid to operate as Distributed Generations (DGs) [1], [2], [3]. Microgrids are usually formed by integrating energy storage devices, Distributed Energy Resources (DERs), and loads [4], [5]. It may operate autonomously as an islanded mode of operation or as a grid-connected mode integrated within the main power grid [6]. Compared to an AC microgrid, a DC microgrid has the easiest control and the highest efficiency due to its immunity from the main issues of an AC microgrid, such as frequency synchronization, inrush currents, and reactive power control [7].

Figure 1 displays a DC microgrid with a single-bus topology, where every converter is connected in parallel. The main control issues that arise in a parallel-connected DC microgrid are current/load sharing among all converters [8], [9] and DC bus voltage regulation [10], [11]. Traditionally, in order to maintain proper current sharing at the primary level, droop control is used [12]. It is constructed by inserting a virtual resistance loop or droop resistance into the primary-level control of a converter [13]. The traditional droop technique has certain limitations [14]. First, the deviation in DC bus voltage due to voltage drop, and second, current sharing accuracy is poor because of uneven line resistances.

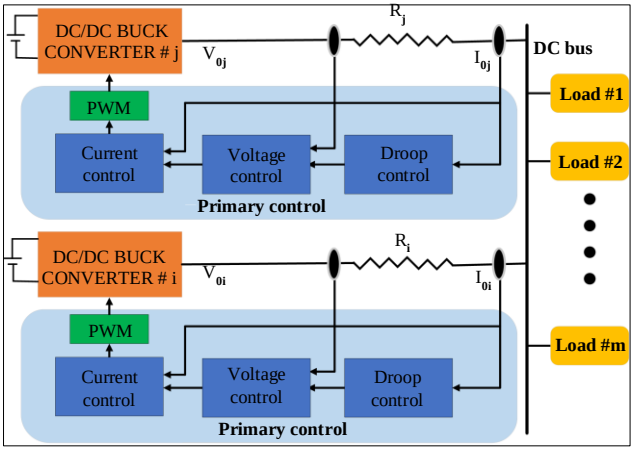

Fig.1 Droop-controlled DC microgrid

To mitigate the limitation of a droop control technique at a primary level, generally, a secondary control technique is required to increase the current sharing accuracy and regulate the voltage of a DC bus [15].

According to the communication techniques used between converters, secondary control systems may be divided into three types: centralized, decentralized, and distributed control [16]. In centralized secondary control, the Microgrid Central Controller (MGCC) must collect all necessary data from each converter and transmit a control signal to every converter through a communication network [17]. The main disadvantages of a centralized secondary control technique are reduced reliability, scalability, and flexibility, as well as susceptibility to a single-point failure [18]. On the contrary, the decentralized control technique is easy to implement without communication but may neither deliver accurate, current sharing nor achieve microgrid global optimisation due to a lack of global information [19].

As per the literature survey, distributed control is used to mitigate the limitations of decentralized and centralized control. It is scalable, flexible, and immune from single-point failure [20]. A distributed control is proposed in the literature to achieve good current-sharing accuracy and voltage regulation. [21], [22]. In [21], a control technique was proposed based on voltage shifting and adaptive droop control. In [22], a variable droop resistance was proposed that is adjusted based on the line resistance.

Recently, consensus algorithm-based secondary control techniques have been the focus of extensive research. Numerous studies have explored distributed sliding mode control [23] and event-triggered based control [20] and analyzed stability with communication delay [24], but they suffer from slow convergence speeds. Although several research works have offered fixed-time or finite-time designs to enhance the system's convergence speed [11], [25], [26], [27], the majority of the relevant papers still use the consensus algorithm. Nevertheless, these required a rigorous mathematical analysis.

This research paper presents a distributed secondary-level control in the DC microgrid based on a Low-Bandwidth Communication (LBC) network. It is built on the current averaging principle to attain good current-sharing accuracy and voltage regulation simultaneously.

The advantages of this technique are simplicity, easiest control, high reliability, flexibility, and reduced communication pressure due to transmitting only one variable over a communication link.

It is capable of handling both resistive loads and Constant Power Loads (CPLs). It also has the plug-and-play capability of the microgrid. The results of the presented technique are verified through the MATLAB/ Simulink software.

2. Formulating Problem and Control Objective

This paper considers an islanded DC microgrid based on a single-bus topology, as displayed in Figure 1. It consists of M loads and N DC/DC converters connected in parallel to a DC bus [28], [29].

Droop control is a conventional approach utilized for current sharing amongst the parallel connected DC sources. First, review the droop control method, discuss its limitations, and then state the control objective,

2.1. Droop Control

When the voltage and current control loops for ith converter, i = 1, 2, ..., N, is appropriately designed, the output voltage V_{0i} is able to follow its reference voltage, V_i^{ref} [29] i.e. $V_{0i} = V_i^{ref}$.

A droop control produces the voltage reference, V_i^{ref} to ensure appropriate current sharing amongst the converters.

$$V_i^{ref} = V_N^* - k_{di} I_{0i} \quad (1)$$

Where V_N^* is the open loop nominal DC bus voltage, k_{di} and I_{0i} is the droop gain and output current of an ith converter. The DC bus voltage V_{Bus} is calculated by the following formula.

$$V_{Bus} = V_{0i} - R_i I_{oi} \quad (2)$$

Where ith transmission line resistance is given by R_i. After that obtain,

$$V_{Bus} = V_N^* - (R_i + k_{di})\, I_{0i} \quad (3)$$

From equation (3),

$$(R_i + k_{di}) I_{0i} = (R_j + k_{dj}) I_{0j}\,, \forall \mathrm{i,j} = 1,2,\ldots,\mathrm{N} \quad (4)$$

So, the current sharing ratio amongst the converters is determined by the sum of the line resistance R_i and the droop gaink_{di}.

$$\frac{I_{0i}}{I_{0j}} = \frac{R_j + k_{dj}}{R_i + k_{di}} \quad (5)$$

Normally, set the droop gain k_{di} is higher than the resistance of a transmission line, R_i , i.e. $k_{di} >> R_i$, hence obtain

$$\frac{I_{0i}}{I_{0j}} = \frac{k_{dj}}{k_{di}} \quad (6)$$

As per the above discussion, accurate, current sharing amongst the converters is accomplished by properly adjusting the droop gain.

2.2. Control Objective

Set the droop gain k_{di} significantly bigger than the line resistance R_i to secure proportional current sharing amongst all converters in parallel connected DC microgrids. But, as per equation (2), a high droop gain k_{di} consequences in a greater voltage drop in voltage of the DC bus V_{Bus} from its nominal voltage V_N^*, indicating poor voltage regulation. So, the control objective of the presented paper is to simultaneously attain good voltage regulation and current sharing amongst all parallel connected converters.

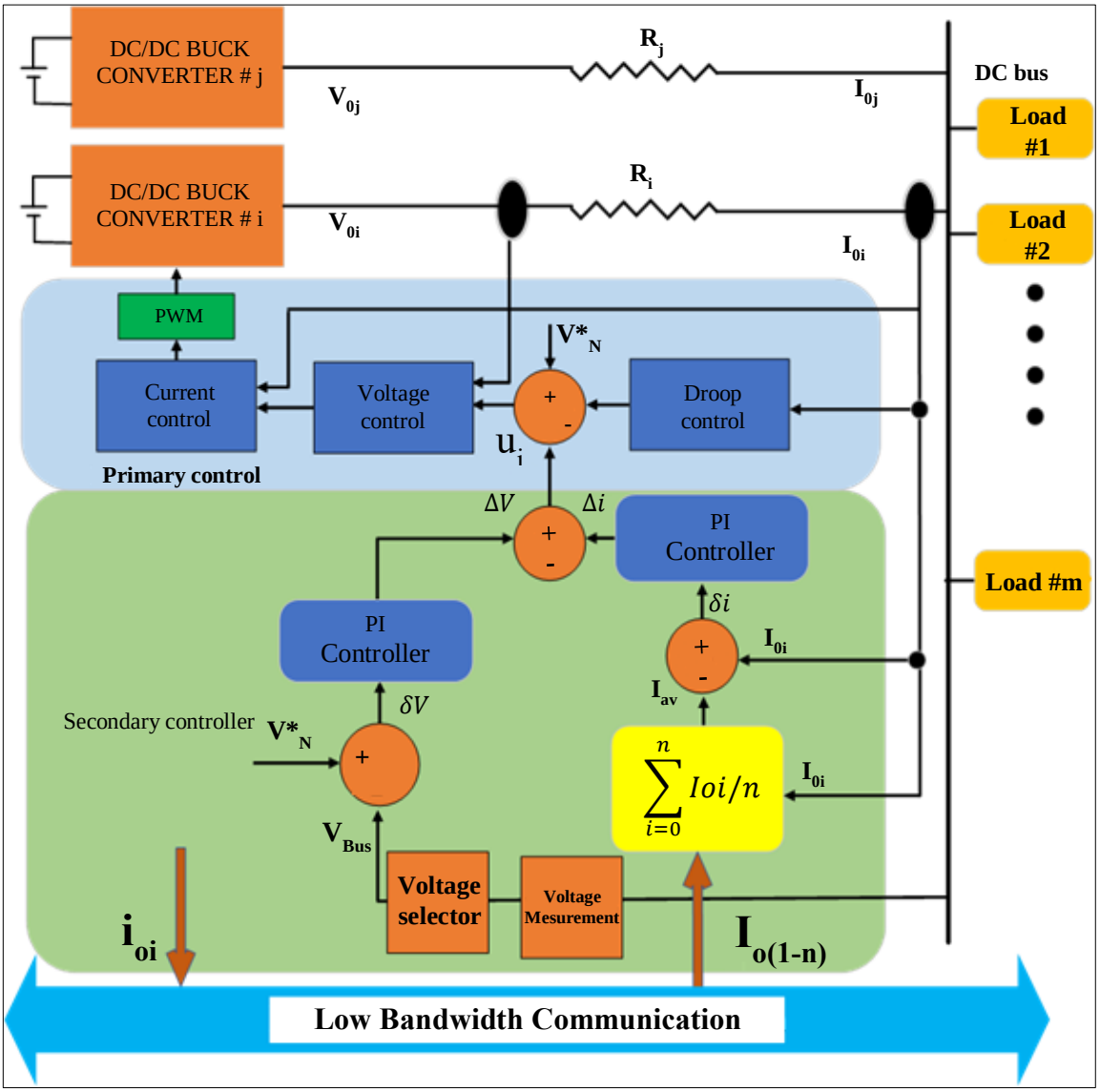

Fig. 2 Presented distributed secondary control.

3. Presented Distributed Secondary Control

To accomplish the above objectives, this paper presents a distributed approach to secondary control techniques. A droop control directly regulates every converter, as displayed in Figure 1. Subsequently, the secondary control signal has to be generated and integrated into the primary control layers. Then equation (1) becomes

$$V_i^{ref} = V_N^* - k_{di} I_{0i} + u_i \qquad (7)$$

Figure 2 displays the block arrangements for the presented secondary-level control techniques. It uses a Controller Area Network (CAN) bus to build a low-bandwidth communication channel, and buck converters are used for the DC-DC interfacing. It contains two distinct levels of control: the primary level and the secondary level. Primary-level control comprises inner-loop current control and voltage control. And outer loop droop control. Every converter's DC output voltage is controlled through inner loop control, and a reference signal for inner loop control is generated by droop

control to secure proper current sharing amongst all the converters.

Every converter output current is transmitted to all other converters via a low-bandwidth communication link. While every converter measures the DC bus voltage, V_{Bus}. If $V_{Bus} \geq V_{BusU}$ then consider a V_{Bus} is equal to V_{BusU} and if $V_{Bus} \leq V_{BusL}$ then consider a V_{Bus} is equal to V_{BusL}, where V_{BusL} and V_{BusU} are the lower and upper limits of a DC bus voltage, respectively. The secondary controller consists of two control loops to generate a secondary control signalu_i. Voltage control loop and average current control loop. The current control loop generates a current signalΔI.

$$\text{The average current, } I_{av} = \frac{1}{N}\sum_{i=1}^{N} I_{0i} \quad (8)$$

$$\text{current error, } \delta_i = I_{av} - I_{0i} \quad (9)$$

$$\text{and } \Delta i = \left(K_{pi} + \frac{K_{ii}}{s}\right)(I_{av} - I_{0i}) \quad (10)$$

The voltage control loop produces a voltage signal ΔV.

$$\text{voltage error, } \delta_v = V_N^* - V_{Bus} \quad (11)$$

$$\text{and } \Delta V = \left(K_{pv} + \frac{K_{iv}}{s}\right)(V_N^* - V_{Bus}) \quad (12)$$

Then, the secondary control signal is,

$$u_i = \left(K_{pv} + \frac{K_{iv}}{s}\right)(V_N^* - V_{Bus}) - \left(K_{pi} + \frac{K_{ii}}{s}\right)(I_{av} - I_{0i}) \quad (13)$$

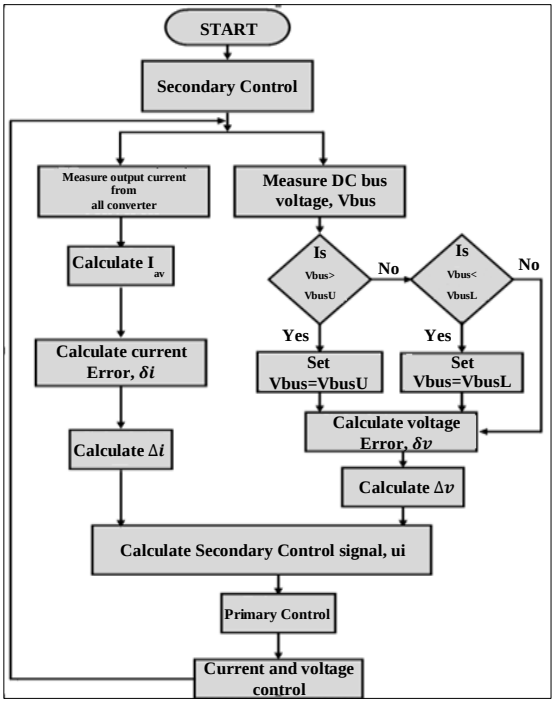

Fig. 3 Flowchart of a presented control technique

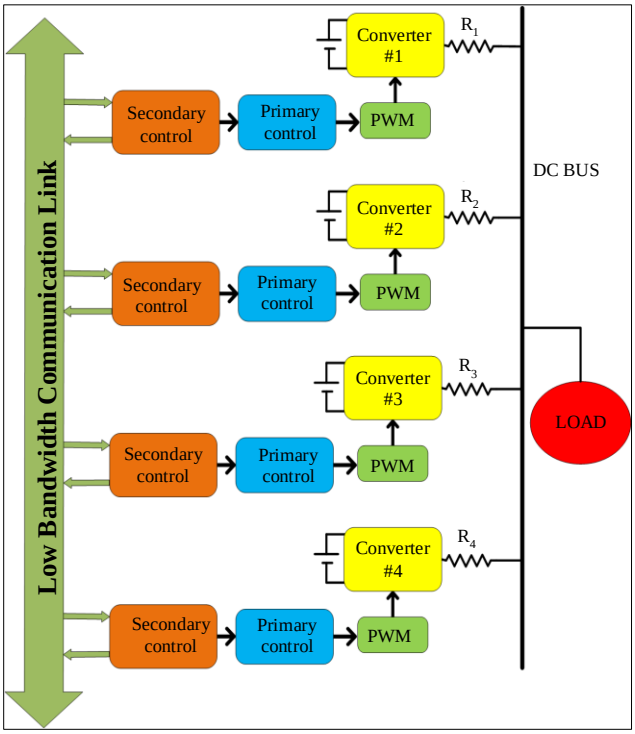

Fig. 4 Simulation block arrangement

Table 1. Parameter of a simulated system

Parameter	Converter#1	Converter#2	Converter#3	Converter#4
Power rating	10 kW	10 kW	20 kW	20 kW
Output voltage	400 Volt	400 Volt	400 Volt	400 Volt
Switching frequency	10 kHz	10 kHz	10 kHz	10 kHz
Inductor	5.28 mH	5.28 mH	2.64 mH	2.64 mH
Capacitor	156.25 µF	156.25 µF	312.5 µF	312.5 µF
Line resistance	0.4 Ω	0.3 Ω	0.2 Ω	0.1 Ω
Droop gain	2	1.5	1	0.5
Secondary voltage loop	K_{pv} = 50	K_{pv} = 50	K_{pv} = 50	K_{pv} = 50
	K_{iv} = 7	K_{iv} = 7	K_{iv} = 7	K_{iv} = 7
Secondary current loop	K_{pc} = 40	K_{pc} = 40	K_{pc} = 40	K_{pc} = 40
	K_{ic} = 7	K_{ic} = 7	K_{ic} = 7	K_{ic} = 7

To simultaneously attain good current-sharing accuracy and voltage regulation, the secondary-level control produces a reference signal for the primary control.

$$V_{0i}^* = V_N^* - k_{di}I_{0i} + \Delta V - \Delta i \quad (14)$$

Figure 3 displays the flowchart of the presented secondary control technique.

4. Simulation Results

A schematic arrangement of the simulation study is displayed in Figure 4. It contains four buck converters, which are parallelly connected to supply a common DC load. The system parameter is displayed in Table 1. In this section, to prove the results of a presented distributed control technique at the secondary level considered the following five case studies using MATLAB/Simulink software: (1) increase in resistive load condition; (2) decrease in resistive load condition; (3) variable resistive load condition; (4) constant power load condition; (5) plug-and-play capability

4.1. Case-1: Increase in Load

The function of a presented distributed secondary control technique is evaluated in this study with regard to an increase in resistive load conditions. The following five steps are used to energize the DC microgrid system:

- **Step-1 (0s–0.2s):** At t = 0s, use a droop control alone in the primary level with a 15 kW load.
- **Step-2 (0.2s–0.5s):** At t = 0.2s, apply the presented distributed secondary control.

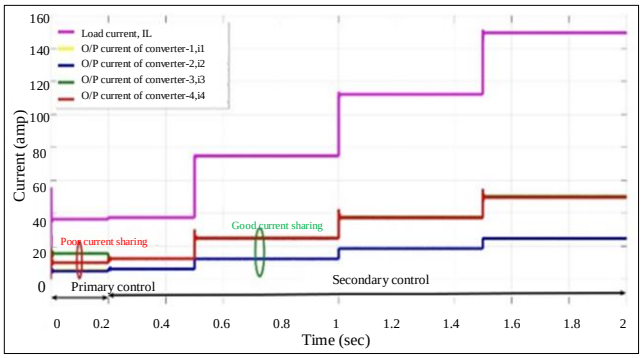

Fig. 5 Current with increasing load

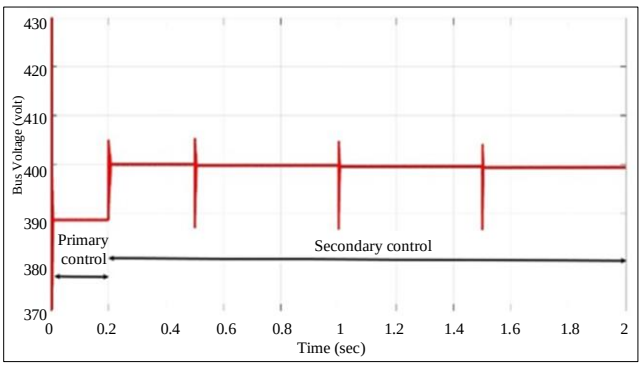

Fig. 6 Bus voltage with increasing load

- **Step-3 (0.5s–1.0s):** At t = 0.5s, apply a 30 kW load.
- **Step-4 (1.0s–1.5s):** At t = 1.0s, apply a 45 kW load.
- **Step-5 (1.5s–2.0s):** At t = 1.5s, apply a 60 kW load.

The Case-1 results are displayed in Figures 5 and 6. As per Figure 5, at the beginning, the first 0.2 s droop control has been applied alone with a 15 kW resistive load; i_1 is around 5.832 A, i_2 is around 4.803 A, i_3 is around 15.71 A, and i_4 is around 10.06 A.

Where converter 1, 2, 3, and 4's output current is represented by i_1, i_2, i_3, and i_4, respectively. Ideally, equal-rated converters must share equal load, so converters 1's and 2's and converters 3's and 4's must share equal load current.

But in this case, converters 1 and 3 share more load current, and converters 2 and 4 share less load current than the ideal load current sharing condition. As a result, the current sharing accuracy is poor.

When the presented secondary level control is applied with a 15 kW resistive load, i_1 is around 6.267 A, i_2 is around 6.21 A, i_3 is around 12.52 A, and i_4 is around 12.54 A. For a 30 kW load, i_1 is around 12.47 A, i_2 is around 12.45 A, i_3 is around 25.11 A, and i_4 is around 24.85 A. For a 45 kW load, i_1 is around 18.77 A, i_2 is around 18.56 A, i_3 is around 37.82 A, and i_4 is around 37.13 A. For a 60 kW load, i_1 is around 24.8 A, i_2 is around 24.77 A, i_3 is around 50.37 A, and i_4 is around 49.67 A. Converters 1's and 2's output current, and converters 3's and 4's output current are almost equal during the condition of an increase in load. Show that the current sharing accuracy is highly improved.

As per Figure 6, when the first 0.2 s droop control is applied alone with a 15 kW resistive load, the DC bus voltage is reduced to around 388.6 V from its nominal voltage of 400 V. When the presented secondary level control is applied, the DC bus voltage V_{Bus} is reinstalled to around 399.9 V.

For a 30 kW load, V_{Bus} is around 399.8 V; for a 45 kW load, V_{Bus} is around 399.6 V; and for a 60 kW load, V_{Bus} is around 399.3 V. prove that DC bus voltage drops by around 0.7 V during the increasing load from 15 kW to 60 kW in a step of 15 kW, indicating good voltage regulation.

4.2. Case-2: Decrease in Load

The function of a presented distributed secondary control technique is evaluated in this study with regard to a decrease in resistive load conditions. The following five steps are used to energize the DC microgrid system:

- **Step-1 (0s–0.2s):** At t = 0s, use a droop control alone in the primary level with a 60 kW load.
- **Step-2 (0.2s–0.5s):** At t = 0.2s, apply the presented distributed secondary control.
- **Step-3 (0.5s–1.0s):** At t = 0.5s, apply a 45 kW load.
- **Step-4 (1.0s–1.5s):** At t = 1.0s, apply a 30 kW load.
- **Step-5 (1.5s–2.0s):** At t = 1.5s, apply a 15 kW load.

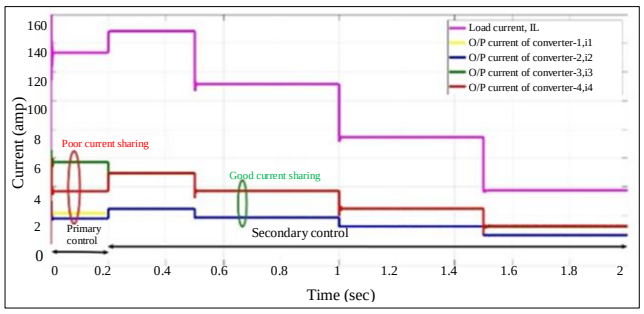

Fig. 7 Current with decreasing load

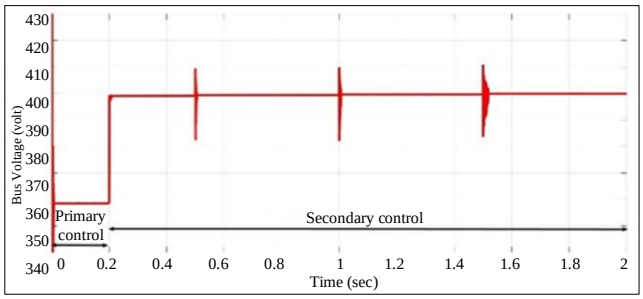

Fig. 8 Bus voltage with decreasing load

The Case-2 results are displayed in Figures 7 and 8. As per Figure 7, at the beginning, the first 0.2 s droop control has been applied alone with a 60 kW resistive load; i_1 is around 21.52 A, i_2 is around 17.87 A, i_3 is around 57.26 A, and i_4 is around 36.76 A. Where converter 1, 2, 3, and 4's output current is represented by i_1, i_2, i_3, and i_4, respectively. Ideally, equal-rated converters must share equal load, so converters 1's and 2's and converters 3's and 4's must share equal load current. But in this case, converters 1 and 3 share more load current, and converters 2 and 4 share less load current than the ideal load current sharing condition. As a result, the current sharing accuracy is poor.

When the presented secondary level control is applied with a 60 kW resistive load, i_1 is around 24.8 A, i_2 is around 24.62 A, i_3 is around 49.64 A, and i_4 is around 49.45 A. For a 45 kW load, i_1 is around 18.57 A, i_2 is around 18.56 A, i_3 is around 37.18 A, and i_4 is around 37.25 A.For a 30 kW load, i_1 is around 12.5 A, i_2 is around 12.46 A, i_3 is around 24.76 A, and i_4 is around 24.83 A. For a 15 kW load, i_1 is around 6.295 A, i_2 is around 6.348 A, i_3 is around 12.12 A, and i_4 is around 12.64 A.

Converters 1's and 2's output current, and converters 3's and 4's output current are almost equal during the condition of a decrease in load. Show that the current sharing accuracy is highly improved.

As per Figure 8, when the first 0.2 s droop control is applied alone with a 60 kW resistive load, the DC bus voltage is reduced to around 358.5 V from its nominal voltage of 400 V. When the presented secondary level control is applied, the DC bus voltage V_{Bus} is reinstalled to around 399.1 V.

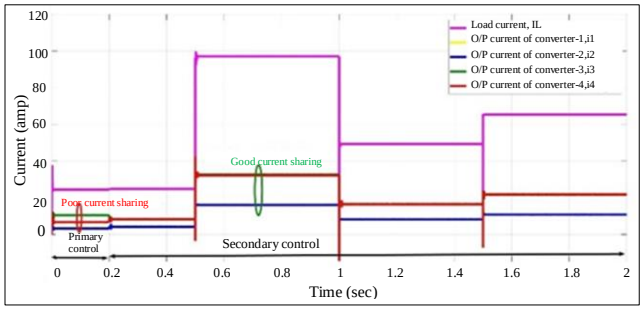

Fig. 9 Current with variable load

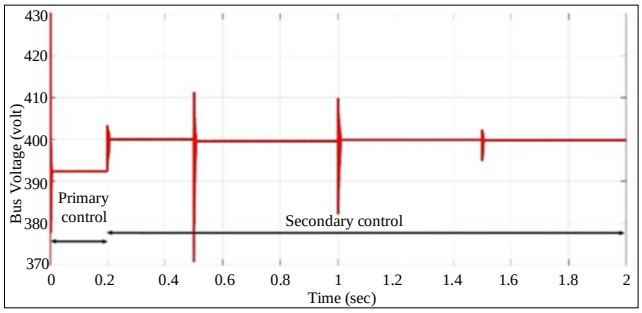

Fig. 10 Bus voltage with variable load

For a 45 kW load, V_{Bus} is around 399.3 V; for a 30 kW load, V_{Bus} is around 399.6 V; and for a 15 kW load, V_{Bus} is around 399.9 V. prove that DC bus voltage increase by around 0.8 V during the decreasing load from 60 kW to 15 kW in a step of 15 kW, indicating good voltage regulation.

4.3. Case-3: Variable Load

The function of a presented distributed secondary control technique is evaluated in this study with regard to a variable resistive load condition. The following five steps are used to energize the DC microgrid system,

Step-1 (0s–0.2s): At t = 0s, use a droop control alone in the primary level with a 10 kW load.

Step-2 (0.2s–0.5s): At t = 0.2s, apply the presented distribution secondary control.

Step-3 (0.5s–1.0s): At t = 0.5s, apply a 40 kW load.

Step-4 (1.0s–1.5s): At t = 1.0s, apply a 20 kW load.

Step-5 (1.5s–2.0s): At t = 1.5s, apply a 26.7 kW load.

The Case-3 results are displayed in Figures 9 and 10. As per Figure 9, at the beginning, the first 0.2 s droop control has been applied alone with a 10 kW resistive load; i_1 is around 3.908 A, i_2 is around 3.262 A, i_3 is around 10.42 A, and i_4 is around 6.771 A. Where converter 1, 2, 3, and 4's output current is represented by i_1, i_2, i_3, and i_4, respectively. Ideally, equal-rated converters must share equal load, so converters 1's and 2's and converters 3's and 4's must share equal load

current. But in this case, converters 1 and 3 share more load current, and converters 2 and 4 share less load current than the ideal load current sharing condition. As a result, the current sharing accuracy is poor.

When the presented secondary level control is applied with a 10 kW resistive load, i_1 is around 4.13 A, i_2 is around 4.014 A, i_3 is around 8.323 A, and i_4 is around 8.364 A. For a 40 kW load, i_1 is around 16.1 A, i_2 is around 16.11 A, i_3 is around 32.61 A, and i_4 is around 32.19 A. For a 20 kW load, i_1 is around 8.167 A, i_2 is around 8.203 A, i_3 is around 16.58 A, and i_4 is around 16.31 A. For a 26.7 kW load, i_1 is around 10.92 A, i_2 is around 10.88 A, i_3 is around 21.93 A, and i_4 is around 21.62 A. Converters 1's and 2's output current, and converters 3's and 4's output current are almost equal during the condition of a variable load. Show that the current sharing accuracy is highly improved.

As per Figure 10, when the first 0.2 s droop control is applied alone with a 10 kW resistive load, the DC bus voltage is reduced to around 392.3 V from its nominal voltage of 400 V. When the presented secondary level control is applied, the DC bus voltage V_{Bus} is reinstalled to around 399.9 V. For a 40 kW load, V_{Bus} is around 399.5 V; for a 20 kW load, V_{Bus} is around 399.8 V; and for a 26.7 kW load, V_{Bus} is around 399.8 V. That proves that the variation in DC bus voltage is around 0.4 V during the variable load condition, indicating good voltage regulation.

4.4. Case-4: Constant Power Load

The function of a presented distributed secondary control technique is evaluated in this study with regard to a constant power load condition. The following three steps are used to energize the DC microgrid system,

- **Step-1 (0s–0.5s):** At t = 0s, apply the presented distribution secondary control with a 15 kW constant power load.
- **Step-2 (0.5s–1.0s):** At t = 0.5s, switch on the 20 kW resistive load in conjunction with constant power load.
- **Step-3 (1.0s–2.0s):** At t = 1.0s, switch off the 20 kW resistive load.

The Case-4 results are displayed in Figures 11 and 12. As per Figure 11, at the beginning, the first 0.5 s When the presented secondary level control is applied with a 15 kW constant power load, i_1 is around 6.224 A, i_2 is around 6.153 A, i_3 is around 12.83 A, and i_4 is around 12.3 A. At t = 0.5 s, a 20 kW resistive load is added to a 15 kW constant power load. Now, i_1 is around 9.574 A, i_2 is around 9.423 A, i_3 is around 19.49 A, and i_4 is around 18.91 A. And at t = 1 s, switch off the 20 kW resistive load. Now, i_1 is around 6.238 A, i_2 is around 6.161 A, i_3 is around 12.81 A, and i_4 is around 12.3 A. Converters 1's and 2's output current and converters 3's and 4's

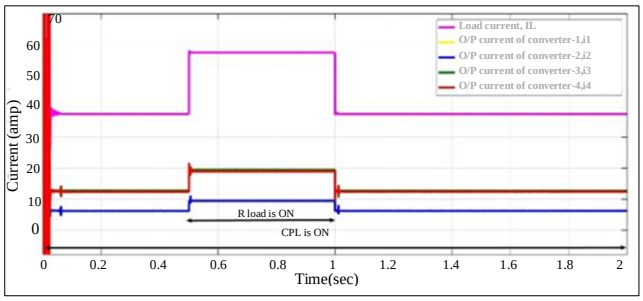

Fig. 11 Current with constant power load

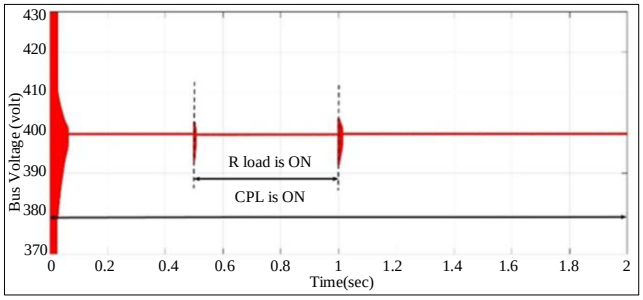

Fig. 12 Bus voltage with constant power load

Output current are almost equal during the condition of a constant power load. Show that the current sharing accuracy is highly improved.As per Figure 12, at the beginning, the first 0.5 s, when the presented secondary level control is applied with a 15 kW constant power load, the DC bus voltage is reduced to around 399.8 V from its nominal voltage of 400 V. At t = 0.5 s, a 20 kW resistive load is added to a 15 kW constant power load. Now, the DC bus voltage is around 399.6 V. And at t = 1 s, switch off the 20 kW resistive load.Now, the voltage of the DC bus is around 399.8 V. That proves that the variation in voltage of the DC bus is around 0.2 V with the constant power load condition, indicating good voltage regulation.

4.5. Case-5: Plug and Play Capability

The function of a presented distributed secondary control technique is evaluated in this study with regard to the plug-and-play capability of a microgrid. The following five steps are used to energize the DC microgrid system,

- **Step-1 At t = 0 s**, apply the presented distribution secondary control with a 4 kW resistive load.
- **Step-2 At t = 0.5 s**, switch off the converter-1
- **Step-3 At t = 1.0 s**, switch on the converter-1
- **Step-4 At t = 1.5 s**, switch off the converter-3
- **Step-5 At t = 2.0 s**, switch on the converter-3

The Case-5 results are displayed in Figures 13 and 14. As per Figure 13, at the beginning, for the first 0.5 s, when the presented secondary level control is applied with a 4 kW resistive load, i_1 is around 1.706 A, i_2 is around 1.652 A, i_3 is

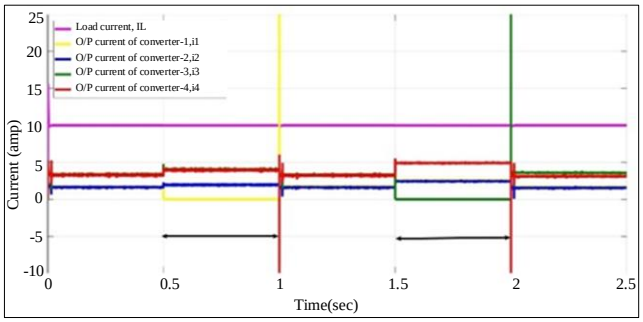

Fig. 13 Current during the switching of a converter

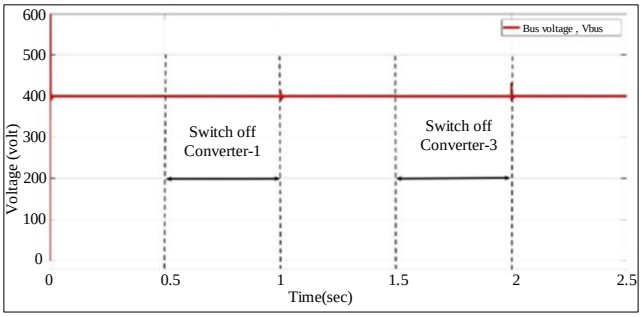

Fig. 14 Voltage during the switching of a converter

Around 3.477 A, and i_4 is around 3.159 A. At t = 0.5 s, converter 1 of a 10 kW is disconnected now; i_1 is 0 A, i_2 is around 1.934 A, i_3 is around 3.986 A, and i_4 is around 4.065 A. At t = 1 s again, converter-1 is connected now; i_1 is around 1.805 A, i_2 is around 1.663 A, i_3 is around 3.333 A, and i_4 is around 3.306 A. At t = 1.5 s, again, converter 3 of 20 kW is disconnected now; i_1 is around 2.681 A, i_2 is around 2.464 A, i_3 is 0 A, and i_4 is around 4.837 A. At t = 2 s, converter-3 is connected again now; i_1 is around 1.698 A, i_2 is around 1.517 A, i_3 is around 3.571 A, and i_4 is around 3.212 A. During the plug-and-play operation of the microgrid, converter-1 from t=0.5 s to 1 s and converter-3 from t = 1.5 s to 2.0 s are disconnected. And then, the remaining converters share the load proportional to their capacity which shows that the current sharing accuracy is highly improved.

As per Figure 14, at the beginning, for the first 0.5 s, when the presented secondary level control is applied with a 4 kW resistive load, the DC bus voltage is around 399.9 V. At t=0.5 s, converter 1 of 10 kW is disconnected now, and the DC bus voltage is around 399.5 V. At t = 1.0 s, converter-1 is connected again, and the DC bus voltage is around 399.9 V. At t = 1.5 s, converter 3 of 20 kW is disconnected now, and the DC bus voltage is around 399.4 V. At t = 2.0 s, the converter-3 is connected again, and the DC bus voltage is around 399.9 V.

This proves that during the plug-and-play operation of a microgrid, a DC bus voltage varies around 0.6 V, indicating good voltage regulation.

5. Conclusion

To overcome the limitations of conventional droop control at the primary level, this paper presents a distributed secondary control using a low-bandwidth communication channel in the DC microgrid. It not only ensures higher current-sharing accuracy but also secures good voltage regulation.

The performance of the presented control technique is validated with an unequal line resistance and variable load. It is capable of handling both resistive loads and Constant Power Loads (CPLs). It also ensures the most important plug-and-play capacity of a DC microgrid. Future research can focus on extending the presented secondary control technique to reduce communication in multi-converter microgrid scenarios.

References:

[1] Xia Chen et al., "Distributed Cooperative Control and Stability Analysis of Multiple DC Electric Springs in a DC Microgrid," *IEEE Transactions on Industrial Electronics*, vol. 65, no. 7, pp. 5611-5622, 2018. [CrossRef] [Google Scholar] [Publisher Link]

[2] Pandla Chinna Dastagiri Goud, and Rajesh Gupta, "Solar PV Based Nano Grid Integrated with Battery Energy Storage to Supply Hybrid Residential Loads using Single-Stage Hybrid Converter," *IET Energy Systems Integration*, vol. 2, no. 2, pp. 161-169, 2020. [CrossRef] [Google Scholar] [Publisher Link]

[3] Satish Kumar Injeti, and Vinod Kumar Thunuguntla, "Optimal Integration of DGs into Radial Distribution Network in the Presence of Plug-In Electric Vehicles to Minimize Daily Active Power Losses and to Improve the Voltage Profile of the System Using Bio-Inspired Optimization Algorithms," *Protection and Control of Modern Power Systems*, vol. 5, no. 1, pp. 1-15,2020. [CrossRef] [Google Scholar] [Publisher Link]

[4] Sandeep Anand, Baylon G. Fernandes, and Josep Guerrero, "Distributed Control to Ensure Proportional Load Sharing and Improve Voltage Regulation in Low-Voltage DC Microgrids," *IEEE Trans Power Electron*, vol. 28, no. 4, pp. 1900–1913, 2013. [CrossRef] [Google Scholar] [Publisher Link]

[5] Babak Abdolmaleki et al., "An Instantaneous Event-Triggered Hz-Watt Control for Microgrids," *IEEE Transactions on Power Systems*, vol. 34, no. 5, pp. 3616-3625 2019. [CrossRef] [Google Scholar] [Publisher Link]

[6] Estefanía Planas et al., "AC and DC Technology in Microgrids: A Review," *Renewable and Sustainable Energy Reviews*, vol. 43, pp. 726-749, 2015. [CrossRef] [Google Scholar] [Publisher Link]

[7] Babangida Modu et al., "DC-Based Microgrid: Topologies, Control Schemes, and Implementations," *Alexandria Engineering Journal*, vol. 70, pp. 61-92, 2023. [CrossRef] [Google Scholar] [Publisher Link]

[8] Waner Wodson A.G. Silva, Thiago R. Oliveira, and Pedro F. Donoso-Garcia, "An Improved Voltage-Shifting Strategy to Attain Concomitant Accurate Power Sharing and Voltage Restoration in Droop-Controlled DC Microgrids," *IEEE Transactions Power Electronics*, vol. 36, no. 2, pp. 2396-2406, 2021. [CrossRef] [Google Scholar] [Publisher Link]

[9] Lantao Xing et al., "Distributed Secondary Control for DC Microgrid with Event-Triggered Signal Transmissions," *IEEE Transactions Sustain Energy*, vol. 12, no. 3, pp. 1801-1810, 2021. [CrossRef] [Google Scholar] [Publisher Link]

[10] Junbin Fang et al., "Secondary Power Sharing Regulation Strategy for a DC Microgrid via Maximum Loading Factor," *IEEE Transactions Power Electronics*, vol. 34, no. 12, pp. 11856-11867, 2019. [CrossRef] [Google Scholar] [Publisher Link]

[11] Qi-Fan Yuan et al., "Distributed Fixed-Time Secondary Control for DC Microgrid via Dynamic Average Consensus," *IEEE Transactions Sustainailable Energy*, vol. 12, no. 4, pp. 2008-2018, 2021. [CrossRef] [Google Scholar] [Publisher Link]

[12] Josep M. Guerrero et al, "Hierarchical Control of Droop-Controlled AC and DC Microgrids - A General Approach Toward Standardization," *IEEE Transactions on Industrial Electronics*, vol. 58, no. 1, pp. 158-172, 2011. [CrossRef] [Google Scholar] [Publisher Link]

[13] M. A. Setiawan, A. Abu-Siada, and F. Shahnia, "A New Technique for Simultaneous Load Current Sharing and Voltage Regulation in DC Microgrids," *IEEE Transactions on Industrial Informatics*, vol. 14, no. 4, pp. 1403-1414, 2018. [CrossRef] [Google Scholar] [Publisher Link]

[14] Zhikang Shuai et al., "Hierarchical Structure and Bus Voltage Control of DC Microgrid," *Renewable and Sustainable Energy Reviews*, vol. 82, pp. 3670-3682, 2018. [CrossRef] [Google Scholar] [Publisher Link]

[15] Minghan Yuan et al., "Hierarchical Control of DC Microgrid with Dynamical Load Power Sharing," *Applied Energy*, vol. 239, pp. 1-11, 2019. [CrossRef] [Google Scholar] [Publisher Link]

[16] Saroja Kanti Sahoo, Avinash Kumar Sinha, and N. K. Kishore, "Control Techniques in AC, DC, and Hybrid AC-DC Microgrid: A Review," *IEEE Journal of Emerging and Selected Topics in Power Electronics*, vol. 6, no. 2, pp. 738-759, 2018. [CrossRef] [Google Scholar] [Publisher Link]

[17] Fei Gao et al., "An Improved Voltage Compensation Approach in a Droop-Controlled DC Power System for the More Electric Aircraft," *IEEE Transactions Power Electronics*, vol. 31, no. 10, pp. 7369-7383, 2016. [CrossRef] [Google Scholar] [Publisher Link]

[18] Anuoluwapo Aluko et al., "Advanced Distributed Cooperative Secondary Control of Islanded DC Microgrids," *Energies (Basel)*, vol. 15, no. 11, 2022. [CrossRef] [Google Scholar] [Publisher Link]

[19] Michele Cucuzzella, Krishna C. Kosaraju, and Jacquelien M. A. Scherpen, "Distributed Passivity-Based Control of DC Microgrids," *Proceedings of 2019 American Control Conference (ACC), Philadelphia, USA*, 2019, pp. 652-657. [CrossRef] [Google Scholar] [Publisher Link]

[20] Zhongwen Li et al., "Distributed Event-Triggered Secondary Control for Average Bus Voltage Regulation and Proportional Load Sharing of DC Microgrid," *Journal of Modern Power Systems and Clean Energy*, vol. 10, no. 3, pp. 678-688, 2022. [CrossRef] [Google Scholar] [Publisher Link]

[21] Rohit Kumar, and Mukesh Kumar Pathak,, "Distributed Droop Control of DC Microgrid for Improved Voltage Regulation and Current Sharing," *IET Renewable Power Generation*, vol. 14, no. 13, pp. 2499-2506, 2020. [CrossRef] [Google Scholar] [Publisher Link]

[22] Rohit Kumar, and Mukesh Kumar Pathak, "Control of DC Microgrid for Improved Current Sharing and Voltage Regulation," *2020 3rd International Conference on Energy, Power and Environment: Towards Clean Energy Technologies*, pp. 1-4, 2021. [CrossRef] [Google Scholar] [Publisher Link]

[23] Michele Cucuzzella et al., "A Robust Consensus Algorithm for Current Sharing and Voltage Regulation in DC Microgrids," *IEEE Transactions on Control Systems Technology*, vol. 27, no. 4, pp. 1583-1595, 2019. [CrossRef] [Google Scholar] [Publisher Link]

[24] Mi Dong. Li Li et al., "Stability Analysis of a Novel Distributed Secondary Control Considering Communication Delay in DC Microgrids," *IEEE Trans Smart Grid*, vol. 10, no. 6, pp. 6690-6700, 2019. [CrossRef] [Google Scholar] [Publisher Link]

[25] Panbao Wang et al., "A Fully Distributed Fixed-Time Secondary Controller for DC Microgrids," *IEEE Transactions on Industry Applications*, vol. 56, no. 6, pp. 6586-6597, 2020. [CrossRef] [Google Scholar] [Publisher Link]

[26] Subham Sahoo, and Sukumar Mishra, "A Distributed Finite-Time Secondary Average Voltage Regulation and Current Sharing Controller for DC Microgrids," *IEEE Transactions on Smart Grid*, vol. 10, no. 1, pp. 282-292, 2019. [CrossRef] [Google Scholar] [Publisher Link]

[27] Subham Sahoo et al., "A Distributed Fixed-Time Secondary Controller for DC Microgrid Clusters," *IEEE Transactions on Energy Conversion*, vol. 34, no. 4, pp. 1997-2007, 2019. [CrossRef] [Google Scholar] [Publisher Link]

[28] Xiao-Kang Liu et al., "Distributed Hybrid Secondary Control for a DC Microgrid via Discrete-Time Interaction," *IEEE Transactions on Energy Conversion*, vol. 33, no. 4, pp. 1865-1875, 2018. [CrossRef] [Google Scholar] [Publisher Link]

[29] Fanghong Guo et al., "Distributed Secondary Control for Power Allocation and Voltage Restoration in Islanded DC Microgrids," *IEEE Transactions on Sustainable Energy*, vol. 9, no. 4, pp. 1857-1869, 2018. [CrossRef] [Google Scholar] [Publisher Link]